DEVELOPMENT AND CHARACTERIZATION OF Ni-P-CARBON BLACK COMPOSITE COATINGS BY ELECTROLESS PLATING ON API 5L X80 PIPELINE STEEL

Mara Cristina Lopes de Oliveira, mara.oliveira@usp.br[1]
Eloana Patrícia Ribeiro, eloana.ribeiro@gmail.com[2]
Renato Altobelli Antunes, renato.antunes@ufabc.edu.br[2]
Olandir Vercino Correa, ovcorrea@ipen.br[3]

[1]Electrocell Ind. Com. De Equip. Elétricos LTDA, CIETEC, Av. Prof. Lineu Prestes, 2242, São Paulo – SP, 05508-900
[2]Universidade Federal do ABC (UFABC), CECS, Av. Dos Estados, 5001, Santo André – SP, 09210-580
[3]Instituto de Pesquisas Energéticas e Nucleares (IPEN/CNEN-SP), Centro de Ciência e Tecnologia de Materiais (CCTM), Av. Prof. Lineu Prestes, 2242, Cidade Universitária, São Paulo – SP, 05508-000

Abstract. *The purpose of the present work was to develop Ni-P-carbon black composite coatings on API 5L X80 pipeline steel substrate using electroless deposition. Three different plating baths were tested, varying the carbon black concentration from 0.25 g.L^{-1} up to 1.0 g.L^{-1}. After deposition, the coatings were solution annealed at 400 ºC for 1h. The corrosion resistance was evaluated in a 3.5 wt.% NaCl solution at room temperature using electrochemical impedance spectroscopy and potentiodynamic polarization curves. Film morphology was assessed by scanning electron microscopy (SEM). Confocal laser scanning microscopy was used to evaluate the surface roughness of the different composite coatings. The coefficient of friction was evaluated using a nanotribometer. The results showed that the corrosion resistance was improved after carbon black incorporation. However, this effect was dependent on the carbon black concentration. Film roughness increased with the carbon black loading as well as the coefficient of friction. Ni-P-carbon black composite coatings showed improved surface properties with respect to the conventional binary Ni-P layer.*

Keywords: *Ni-P-carbon black coating, electroless deposition, wear, corrosion, API 5L X80 pipeline steel*

1. INTRODUCTION

Autocatalytic Ni-P coatings are traditionally employed as a wear and corrosion resistant layer to protect metallic materials against degradation in a variety of applications (Sageghzadeh-Attar et al, 2016). There is, though, a growing need for improved surfaces to withstand increasingly harsh environments in the petrochemical, oil and gas and cutting tool industries. Incorporation of nanometric particles into Ni-P matrix is an interesting route for enhancing its surface properties (Walsh and Leon, 2014; Islam et al., 2015). Carbon black is relatively cheap filler that is often employed as conductive filler for enhancing the electrical conductivity of polymeric matrices composites (Adloo et al, 2016; Chen et al., 2017). Although not as usual as for bulk polymer-based composites, carbon black particles have also been reported as fillers for electroless Ni-P coatings. Liu et al. (2010), for instance, have developed Ni-P-carbon composite coatings by electroless deposition with the aim of obtaining a low infrared emissivity layer for polymeric substrate. It is not explored, though, as a protective layer against corrosion and wear of metallic substrates.

Pipeline steels used in the oil and gas industry are prone to internal corrosion in contact with either acidic or alkaline based electrolytes (Finsgar and Jackson, 2014; Khalaj and Khalaj, 2016). Allahkaram et al. (2011) proposed the use of Ni-P coatings as a viable protective method against internal corrosion of pipeline steels. Moreover, they highlighted the need for further improving the surface properties of the Ni-P films by incorporating nanoparticles such as Al_2O_3, SiO_2 and SiC. The role of nanoparticles in composite Ni-P films as a corrosion reducing agent is often related to the filling of small pores in the coating structure, thus improving its compactness and reducing the penetration of corrosive species from the electrolyte (Lin et al., 2006). Due to its nanometric dimensions, carbon black particles could be explored as potential reinforcement for electroless Ni-P coatings to protect pipeline steels against corrosion. Furthermore, the lubricant effect of carbon black (Brostow et al., 2005) has been reported for polymeric composites but is not studied for composite metallic films.

In this respect, the aim of the present work was to prepare composite Ni-P-carbon black coatings by electroless deposition on API 5L X80 pipeline steel substrates. The films were characterized with respect to corrosion resistance, morphology and friction characteristics. The electrochemical behavior was assessed by electrochemical impedance spectroscopy and potentiodynamic polarization tests. The film morphology was examined using scanning electron microscopy and the friction behavior was evaluated by dry sliding tests in a nanotribometer.

2. EXPERIMENTAL PROCEDURE

2.1. Materials and coating preparation

The substrate for electroless deposition was API 5L X80 pipeline steel plate (in wt%: 0.04% C, 1.75% Mn, 0.20% Si, 0.02% P, 0.002% S, 0.065% Nb, 0.025% Al, 0.11% Cr, 0.025% V and balance Fe) with dimensions 300 x 200 x 20 mm. The material was kindly provided by Usiminas (Brazil). The as-received material was cut into small rectangular pieces with dimensions 30 x 20 x 5 mm. These parts were used as substrates for coating preparation. Surface preparation before deposition consisted of grinding with SiC paper up to grit 1200, followed by cleaning with alcohol, rinsing with deionized water and drying in a warm air stream provided by a heat gun.

The base composition for Ni-P plating bath is shown in Tab. 1. The chemicals for electroless deposition were pure analytical grade reagents. Carbon black (CB) particles (Vulcan XC 72 Cabot Corporation) were added with three different concentrations 0.25 $g.L^{-1}$, 0.50 $g.L^{-1}$ and 1.0 $g.L^{-1}$. These films are designated as CB1, CB2 and CB3 throughout the text. Magnetic stirring was employed during deposition to disperse the nanometric carbon black particles. The total deposition time was 2 h. Before deposition, alkaline cleaning was carried out in a 10 wt.% NaOH solution at 50 °C for 10 min. Next, the samples were washed with deionized water. Surface activation was, then, performed by immersing the samples in 50% vol. H_2SO_4 solution at room temperature for 30 s. The samples were washed again with deionized water and finally immersed in the Ni-P-CB plating bath. After deposition, the samples were thoroughly washed with deionized water and dried in a warm air stream using a heat gun. Subsequently, the as-deposited samples were subjected to annealing heat treatment in a tubular furnace at 400 °C for 1 h under argon atmosphere. This heat treatment is frequently employed for Ni-P films obtained by electroless deposition in order to promote the precipitation of nickel phosphides that increase the hardness of the as-deposited layers (Balaraju et al., 2006). The heat treated samples were, then, characterized according to the procedure described in section 2.2.

Table 1. Composition and operating conditions of the Ni-P plating bath.

$NiSO_4.6H_2O$	
$Na_2H_2PO_2.H_2O$	
$Na_3C_6H_5O_7.2H_2O$	
$(NH_4)_2SO_4$	
$Na_2WO_4.2H_2O$	
pH	9.0
Temperature	88 ºC
Magnetic stirring	

2.2 Coating characterization

Coating morphology and roughness were examined using scanning electron microscopy (SEM – Hitachi TM3000) and confocal laser scanning microscopy (CLSM – Olympus LEXT OLS4100), respectively. Friction characteristics were assessed by dry sliding reciprocating wear tests using NTR^2 Nanotribometer (Anton Paar). The tests were conducted using a 2 mm-diameter chromium steel ball as counter body, applying a normal load of 20 mN, frequency of 2 Hz and wear track amplitude of 1.5 mm. The variation of the coefficient of friction as a function of the sliding distance was registered during 30 minutes.

Corrosion tests were carried out using a conventional three-electrode cell configuration consisting of a platinum wire as auxiliary electrode, Ag/AgCl as reference and the coated API 5L X80 samples as the working electrodes. Electrical contact was provided by copper wire firmly adhered at the back of the coated samples. The area exposed to the electrolyte was approximately 2.0 cm^2. The tests were conducted in a 3.5 wt.% NaCl solution at room temperature. Firstly, the open circuit potential was monitored for 1 h in order to ensure a steady state condition. Next, electrochemical impedance spectroscopy (EIS) measurements were carried out at the OCP in the frequency range from 100 kHz to 10 mHz with an amplitude of the perturbation signal of 10 mV (rms) and an acquisition rate of 10 points per decade. Right after the EIS measurements, the samples were subjected to potentiodynamic polarization from -300 mV versus the OCP up to 1.0 $V_{Ag/AgCl}$ with a sweep rate of 1 $mV.s^{-1}$. The tests were performed in triplicate.

3. RESULTS AND DISCUSSION

3.1 Surface morphology and roughness

SEM micrographs of the conventional Ni-P and Ni-P-CB coatings annealed at 400 °C for 1 h are shown in Fig. 1. The morphology is predominantly nodular, apart from the carbon black concentration in the plating bath. By increasing CB particles some defective regions proliferated in the surface as can be seen in Figs. 1b, 1c and 1d. These regions are progressively more frequent as the CB concentration increases and are probably related to agglomeration sites of the nanosized filler particles. The formation of agglomerates is frequently reported for nanometric particles such as the CB material used in the present as a result of strong interparticle interaction due to surface charges (Enríquez et al, 2014). As a consequence, corrosion resistance can be adversely affected, depending on the compactness of the deposited layer (Christopher et al, 2015). In spite of such undesirable aspect, the films were mostly compact and completely covered the substrate surface.

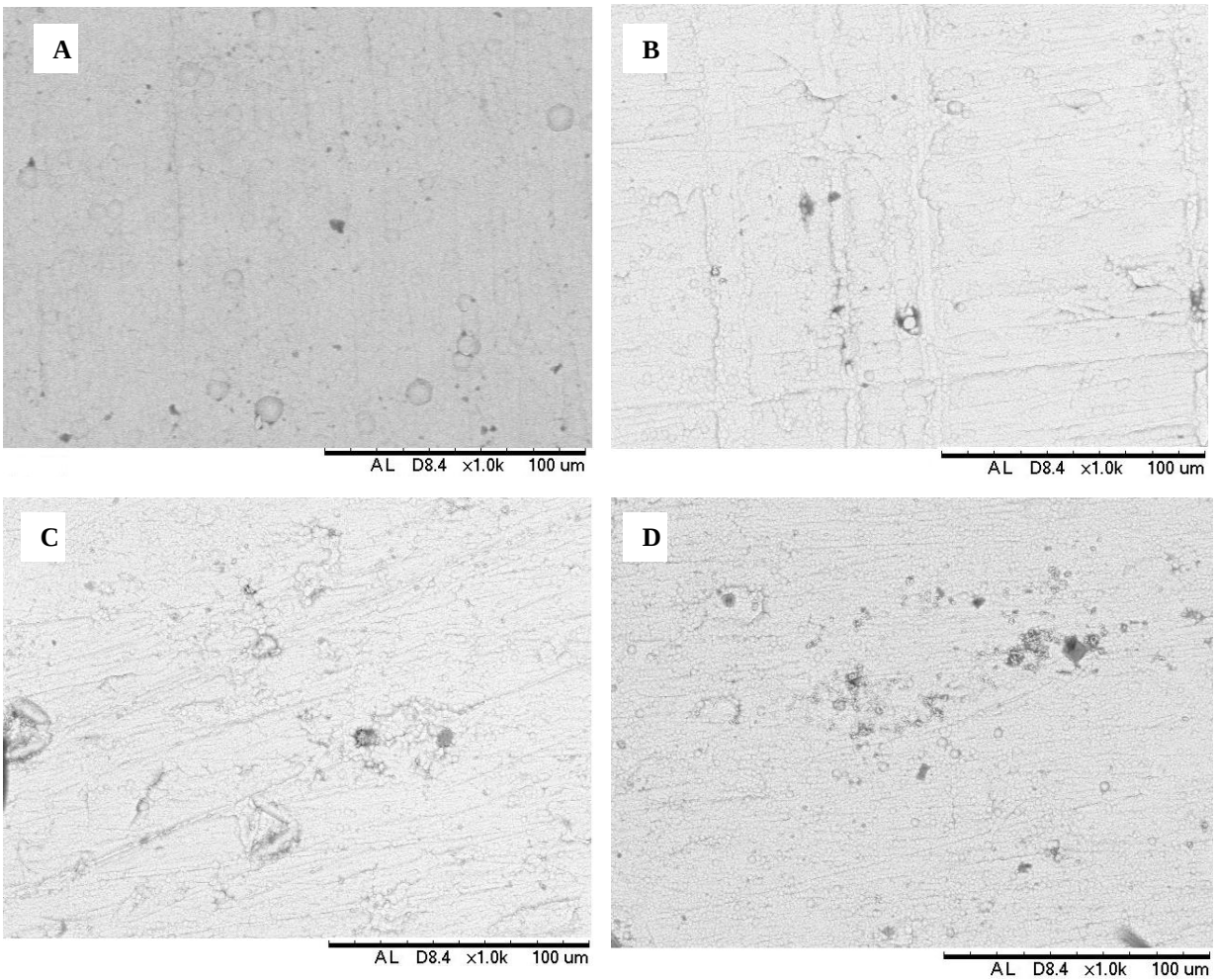

Figure 1. SEM micrographs of the Ni-P-CB coatings after annealing at 400 °C for 1 h: a) Ni-P; b) CB1; c) CB2; d) CB3.

Representative 3D CLSM images of the Ni-P and Ni-P-CB coatings are shown in Fig. 2. The corresponding transverse profile is also displayed. Surface roughness was assessed using these results. The roughness results are expressed using the parameter Ra that corresponds to the arithmetic average roughness of surface and is widely used to characterize the surface profile of engineering materials (De Oliveira et al., 2016). The values of Ra indicate that the incorporation of carbon black particles in the Ni-P coatings increased surface roughness. This can be also visually inferred from the CLSM images shown in Fig. 2 and is confirmed by the surface profiles presented along with the 3D images. The increased roughness of the Ni-P-CB coatings in comparison with the conventional Ni-P can be due to the migration of CB particles to the coating surface as a result of agglomeration regions. It is noteworthy that the roughness of the higher CB loadings coatings (CB2 and CB3) is slightly superior to the low loading CB1 film. Surface roughness is an important characteristic for the friction properties of coatings. Next section deals with this subject.

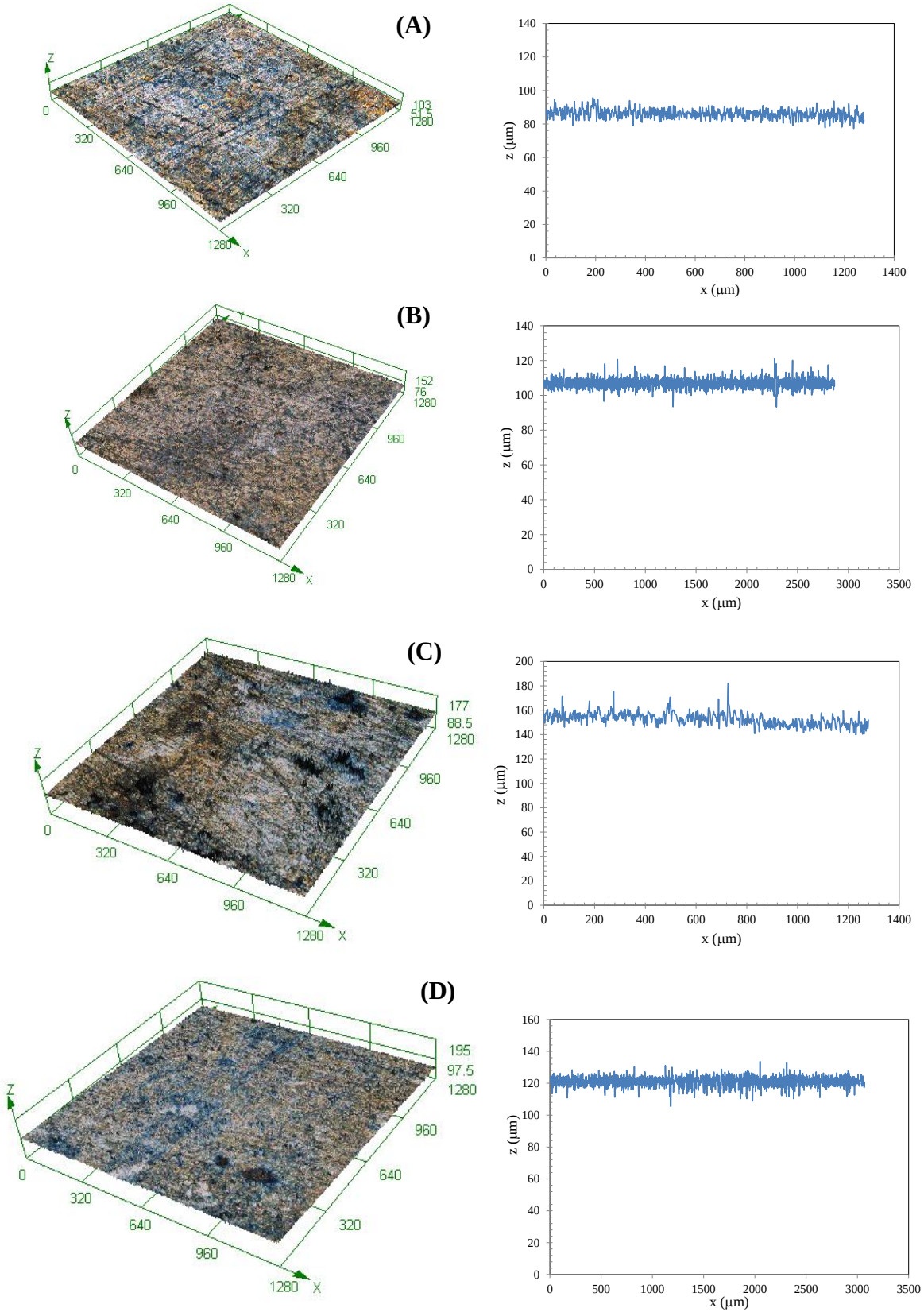

Figure 2. 3D CLSM images and the corresponding transverse profile of: a) Ni-P; b) CB1; c) CB2 and d) CB3 coatings.

Table 2. Surface roughness of the Ni-P and Ni-P-CB coatings.

Coating	Ra (μm)
Ni-P	0.68
CB1	2.04
CB2	2.62
CB3	2.27

3.2 Friction properties

Plots of the variation of the coefficient of friction (COF) with the sliding distance during reciprocating wear tests of Ni-P and Ni-P-CB coatings are shown in Fig. 3.

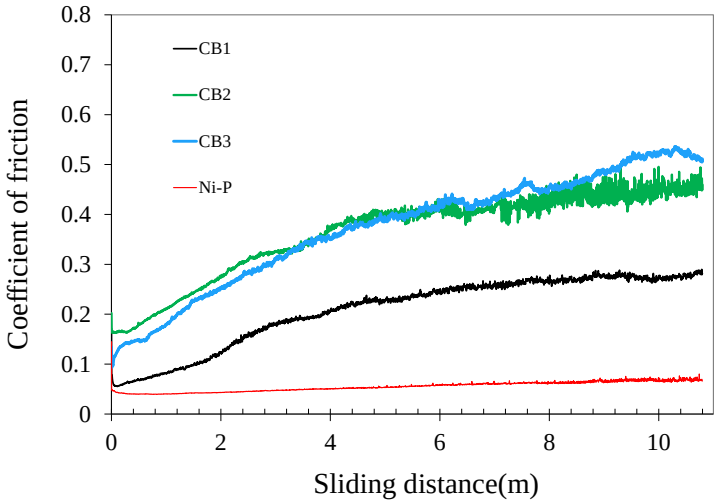

Figure 3. Plots of the variation of the coefficient of friction (COF) with the sliding distance during reciprocating wear tests of Ni-P and Ni-P-CB coatings.

The COF of the conventional Ni-P coating presented a smooth variation and the lowest values during the reciprocating wear test. The plots of the Ni-P-CB coatings increase in the beginning of the test and show a continuous increasing up to the test end. The final COF value was higher for the CB2 and CB3 coatings which presented the highest surface roughness according to the data displayed in Tab. 2. The Ni-P film, in turn, has a low roughness in comparison with the composite Ni-P-CB coatings whereas CB1 has an intermediate roughness. In this respect, the variation of the COF values would reflect the surface roughness of the deposited layers. This behavior was expected, since there are several reports in the literature indicating that the frictional properties and surface roughness of different coatings are directly correlated. COF value tends to decrease as the coating surface becomes smoother (Parthasarathi et al., 2013).

3.3 Electrochemical tests

3.3.1 EIS measurements

Nyquist plots of the uncoated API 5L X80 substrate and Ni-P-CB coatings obtained after 1 h of immersion in 3.5 wt.% NaCl solution at room temperature are shown in Fig. 4. The inset in Fig. 4 shows the plots with expanded scale to more clearly resolve the high frequency domain. All the samples presented one capacitive loop that flattens in the low frequency region of the Nyquist plots. As observed in the inset, the uncoated substrate presents one single capacitive loop with a small diameter. The diameter of the capacitive loop is related to the corrosion resistance of the electrode (Zucchi et al., 2006). In this respect, the results shown in Fig. 4 indicate that CB1 presents higher corrosion resistance than CB2 and CB3.

The impedance values are much higher for the coated samples in comparison with the bare substrate. The lower corrosion resistance of CB2 and CB3 could be ascribed to the morphological features revealed by SEM micrographs. As observed in Fig. 1, a tendency of particle agglomeration was detected for the high-CB concentration coatings CB2 and CB3, thus forming defective regions on the film surfaces. This trend was less marked for CB1. The barrier effect against corrosion is greatly affected by the coating compactness and integrity. Cracks and pores would act as preferential pathways for electrolyte penetration, decreasing the electrode impedance and hampering its corrosion resistance (Lei et al., 2016). The more spread defective regions on the surface of CB2 and CB3 coatings would lead to the smaller size of the capacitive loop in the Nyquist plots, thus reflecting their less effective barrier effect against corrosion of the underlying substrate.

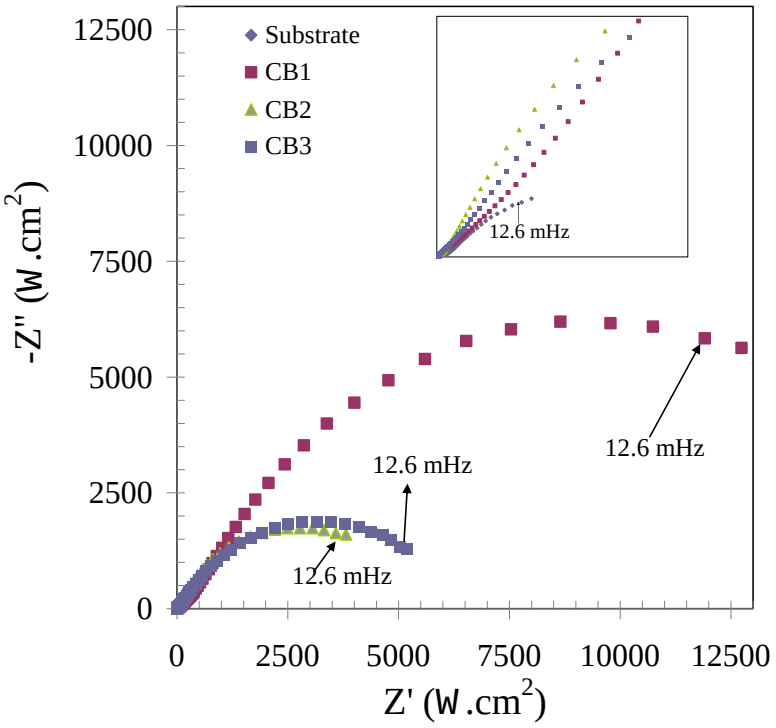

Figure 4. Nyquist plots of the uncoated API 5L X80 substrate and Ni-P-CB coatings in 3.5 wt.% NaCl solution at room temperature.

3.3.2 Potentiodyanamic polarization

The electrochemical behavior of the Ni-P-CB coated API 5L X80 steel was further characterized by potentiodynamic polarization. The polarization curves were obtained right after the EIS measurements. The results are shown in Fig. 5. corrosion potential (Ecorr) and corrosion current density (icorr) values were determined from the polarization curves by the Tafel extrapolation method, considering only the cathodic branches. The results are displayed in Tab. 3. The bare substrate presents the lowest E_{corr} and highest i_{corr} values, indicating its susceptibility to corrosion. The corrosion potential is an indication of the thermodynamic stability of the electrode surface. The more negative the value of E_{corr}, the lowest the electrode stability (Geng et al., 2014; Hu et al., 2017). The corrosion potential was shifted to less negative values after electroless deposition. The Ni-P-CB coatings presented the noblest E_{corr} values when compared to the conventional Ni-P film. The polarization curves of the Ni-P-CB coatings were characterized by the presence of a stable passive range whereas the Ni-P and uncoated substrate samples did not present passive regions. The lower anodic current densities of the Ni-P-CB coatings point to an improved dissolution resistance as the potential increases.

The highest corrosion resistance was observed for the CB1 coating, as denoted by its lowest i_{corr} value. This result is in agreement with the findings from the EIS measurements. The corrosion behavior is, therefore, markedly influenced by coating morphology. The defective regions on the surface of CB2 and CB3 coatings (Figs. 1c and 1d) lead to an increased corrosion rate with respect to the CB1 samples, as denoted by the higher values of i_{corr}. Hence, particle agglomeration during deposition affects the protective character of Ni-P-CB coatings. The electrochemical tests were sensitive to this phenomenon that is apparently more easily controlled when the CB concentration is 0.25 $g.L^{-1}$. Higher loadings enhanced the formation of coating defects and hampered the corrosion properties of the deposited layers.

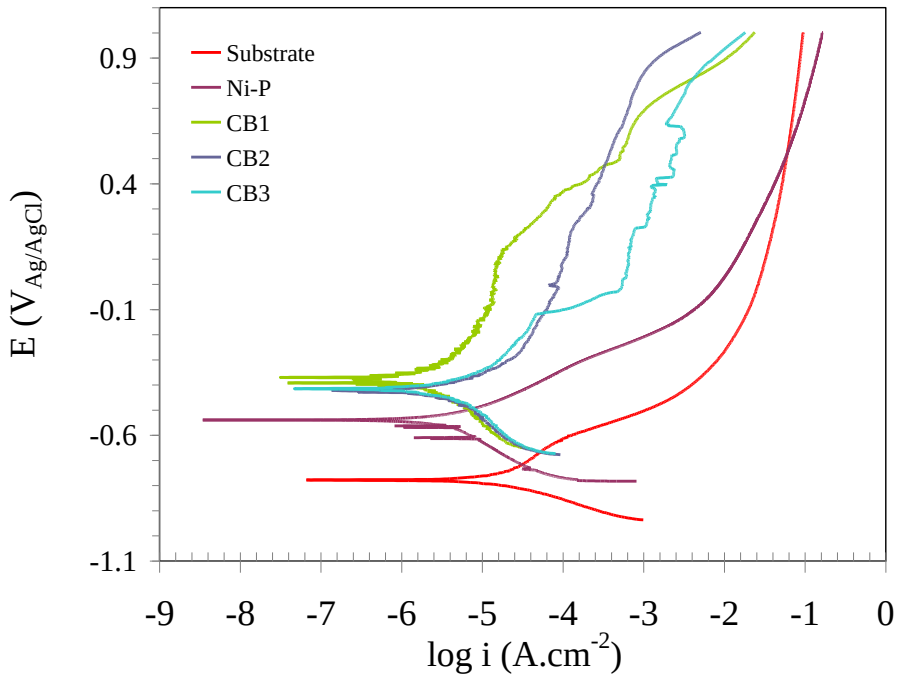

Figure 5. Potentiodynamic polarization curves of the uncoated substrate, Ni-P and Ni-P-CB coatings obtained in 3.5 wt.%NaCl solution at room temperature.

Table 3. Electrochemical parameters determined from the potentiodynamic polarization curves.

Sample	E_{corr} ($mV_{Ag/AgCl}$)	i_{corr} ($\mu A.cm^{-2}$)
Substrate	-778	203
Ni-P	-540	4.17
CB1	-392	2.66
CB2	-421	3.63
CB3	-415	4.15

4. CONCLUSIONS

Ni-P-carbon black composite coatings were successfully produced by electroless deposition. The coating morphology was dependent on the CB concentration in the plating bath. Coatings defects were formed as a result of CB particles agglomeration during deposition. The surface roughness was affected. Smooth surfaces gave rise to lower coefficients of friction. The corrosion behavior was affected as well. The presence of surface defects decreased the corrosion resistance. The best protective effect was obtained by the coating produced in the plating bath with carbon black concentration of 0.25 $g.L^{-1}$.

5. ACKNOWLEDGEMENTS

The authors are thankful to Usiminas for kindly providing the API 5L X80 plate used in the present work and to CNPq (Process 470944/2013-7) for the financial support.

6. REFERENCES

Adloo, A., Sadeghi, M., Masoomi, M. and Pazhooh, H.N., 2016, "High performance polymeric bipolar plate based on polypropylene/graphite/graphene/nano-carbon black composites for PEM fuel cells", Renewable Energy, Vol. 99, pp. 867-874.

Allahkaram, S.R., Nazari, M.H., Mamaghani, S. and Zarebidaki, A., 2011, "Characterization and corrosion behavior of electroless Ni-P/nano-SiC coating inside the CO_2 containing media in the presence of acetic acid", Materials and Design, Vol. 32, pp. 750-755.

Balaraju, J.N., Jahan, S.M. and Rajam, K.S., 2006, "Studies on autocatalytic deposition of ternary Ni-W-P alloys using nickel sulphamate bath", Surface & Coatings Technology, Vol. 201, pp. 507-512.

Brostow, W., Keselman, M., Mironi-Harpaz, I., Narkis, M. and Peirce, R., 2005, "Effects of carbon black on tribology of blends of poly(vinylidene fluoride) with irradiated and non-irradiated ultrahigh molecular weight polyethylene", Polymer, Vol. 46, pp. 5058-5064.

Chen, J., Cui, X., Sui, K., Zhu, Y. and Jiang, W., 2017, "Balance the electrical properties and mechanical properties of carbon black filled immiscible polymer blends with a double percolation structure", Composites Science and Technology, Vol. 140, pp. 99-105.

Christopher, G., Kulandainatha, M.A. and Harichandran, G., 2015, "Comparative study of effect of corrosion on mild steel with waterborne polyurethane dispersion containing graphene oxide versus carbon black nanocomposites", Progress in Organic Coatings, Vol. 89, pp. 199-211.

De Oliveira, A.N., Oliveira, M.C.L., Ríos, C.T. and Antunes, R.A., 2016, "The effect of mechanical polishing and finishing on the corrosion resistance of AISI 304 stainless steel", Corrosion Engineering, Science and Technology, Vol. 51, pp. 416-428.

Enríquez, E., de Frutos, J., Fernández, J.F. and de la Rubia, M.A., 2014, "Conductive coatings with low carbono-black contente by adding carbon nanofibers", Composites Science and Technology, Vol. 93, pp. 9-16.

Finsgar, M. and Jackson, J., 2014, "Application of corrosion inhibitors for steels in acidic media for the oil and gas industry: A review", Corrosion Science, Vol. 86, pp. 17-41.

Geng, J., Teng, X, Zhou, G., Leng, J. and Zhao, D., 2014, "Influence of in situ synthesized TiC on thermal stability and corrosion behavior of Zr60Cu10Al15Ni15 amorphous composites", Physica B, Vol. 436, pp. 47-53.

Hu, L.F., Li, J., Tao, Y.F. and Lv, Y.H., 2017, "Corrosion behaviors of TiNi/Ti2Ni matrix coatings in the environment rich in Cl ions", Surface & Coatings Technology, Vol. 311, pp. 295-306.

Islam, M., Azhar, M.R., Fredj, N., Burleigh, T.D., Oloyede, O.R., Almajid, A. and Shah, S.J., 2015, "Influence of SiO_2 nanoparticles on hardness and corrosion resistance of electroless Ni-P coatings", Surface & Coatings Technology, Vol. 261, pp. 141-148.

Khalaj, G. and Khalaj, M.-J., 2016, "Investigating the corrosion of the heat-affected zones (HAZs) of API-X70 pipeline steels in aerated carbonate solution by electrochemical methods", International Journal of Pressure Vessels and Piping, Vol. 145, pp. 1-12.

Lei, L., Shi, J., Wang, X., Liu, D. and Xu, H., 2016, "Microstructure and electrochemical behavior of cerium conversion coating modified with silane agent on magnesium substrates", Applied Surface Science, Vol. 376, pp. 161-171.

Lin, C.J., Chen, K.C. and He, J.L., 2006, "The cavitation erosion behavior of electroless Ni-P-SiC composite coating", Wear, Vol. 261, pp. 1390-1396.

Liu, X., Wu, C. and Wang, X., 2010, "Synthesis, characterization, and infrared-emissivity study of Ni-P-CB nanocomposite coatings by electroless process", Journal of Coating Technology and Research, Vol. 7, pp. 659-664.

Parthasarathi, N.L., Borah, U. and Albert, S.K., 2013, Correlation between coefficient of friction and surface roughness in dry sliding wear of AISI 316L (N) stainless steel at elevated temperatures", Computer Modelling and New Technologies, Vol. 17, pp. 51-63.

Sadeghzadeh-Attar, A., Ayubikia, G. and Ehteshamzadeh, M., 2016, "Improvement in tribological behavior of novel sol-enhanced electroless Ni-P-SiO2 nanocomposite coatings", Surface & Coatings Technology, Vol. 307, pp. 837-848.

Walsh, F.C. and de León, C.P., 2014, "A review of the electrodeposition of metal matrix composite coatings by inclusion of particles in a metal layer: an established and diversifying coatings technology", Transactions of the Institute of Metal Finishing, Vol. 92, pp. 83-98.

Zucchi, F., Grassi, V., Frignani, A., Monticelli, C. and Trabanelli, G., 2006, "Electrochemical behaviour of a magnesium alloy containing rare earth elements", Journal of Applied Electrochemistry, Vol. 36, pp. 195-204.

7. RESPONSIBILITY NOTICE

The authors are the only responsible for the printed material included in this paper.